Water Activity and the Challenge for Life on Early Mars

Nicholas J. Tosca, *et al.*

Science **320**, 1204 (2008);
DOI: 10.1126/science.1155432

Science (print ISSN 0036-8075; online ISSN 1095-9203) is published weekly, except the last week in December, by the American Association for the Advancement of Science, 1200 New York Avenue NW, Washington, DC 20005.

GeoEng_Large_Aerosol and by more than 30 years for GeoEng_Small_Aerosol (Fig. 3B). Assuming a vertical expansion of the ozone hole, the first stage of recovery would be delayed by another 30 years for both cases (Fig. 3C). The recovery of Antarctic ozone to conditions that prevailed in 1980 would be delayed until the last decade of this century by geoengineering, assuming no vertical expansion of the ozone loss region (Fig. 3B). However, if the vertical extent of the ozone hole were to increase, this stage of recovery would not occur within this century (Fig. 3C).

Our estimates of the risk of geoengineering do not consider several important effects. A possible consequence of a stratospheric sulfur injection, which was not considered here, is a strengthening of the polar vortex, because of the stronger temperature gradient between high and low latitudes caused by enhanced stratospheric aerosol (*20*). This could increase the frequency of cold polar winters, leading to even greater ozone loss than estimated. On the other hand, volcanic aerosols might result in dynamic instabilities, causing earlier major stratospheric warming at the end of Arctic winters, which results in smaller PACl and therefore less ozone loss. Also, enhanced sulfate aerosols could suppress denitrification in the polar vortices in a manner that might affect the linear relation between ozone loss and PACl. Enhanced ozone loss through geoengineering would also likely result in a thinning of the ozone layer at mid-latitudes due to the export of polar processed air, as observed during the period of rising halogen loading (1979 to 1995) (*21*). Further, the enhanced stratospheric aerosol levels would disturb ozone photochemistry in mid-latitudes, resulting from the suppression of stratospheric NO_x, leading to even further ozone depletion (*22*). Additional uncertainty results from our use of idealized aerosol size and perturbation. Finally, the impact on ozone of any future major volcanic eruption would likely exceed, by large amounts, the ozone loss that was observed after the eruption of Mount Pinatubo and El Chichón, because additional volcanic aerosols will be acting on an already perturbed stratospheric SAD layer. Comprehensive chemistry–climate model simulations, considering these effects and perhaps others, are needed to fully evaluate the impact of geoengineering on atmospheric ozone.

A substantial increase of stratospheric sulfate aerosol densities caused by various geoengineering approaches will likely result in strongly enhanced chemical loss of polar ozone during the next several decades, especially in the Arctic. The expected recovery of the Antarctic ozone hole due to a reduction in stratospheric halogen loading, brought about by the implementation of the Montreal Protocol, could be delayed by between 30 and 70 years by the aerosol perturbation associated with geoengineering.

References and Notes

1. P. J. Crutzen, *Clim. Change* **77**, 211 (2006).
2. P. J. Rasch, P. J. Crutzen, D. B. Coleman, *Geophys. Res. Lett.* **35**, L02809 (2008).
3. T. M. L. Wigley, *Science* **314**, 452 (2006).
4. D. A. Randall *et al.*, in *Climate Change 2007: The Physical Science Basis. Contribution of Working Group I to the Fourth Assessment Report of the Intergovernmental Panel on Climate Change*, S. Solomon *et al.*, Eds. (Cambridge Univ. Press, Cambridge, 2007), chap. 8.
5. A. Tabazadeh, K. Drdla, M. R. Schoeberl, P. Hamill, O. B. Toon, *Proc. Natl. Acad. Sci. U.S.A.* **99**, 2609 (2002).
6. S. Tilmes *et al.*, *Atmos. Chem. Phys.* **8**, 1897 (2008).
7. S. Solomon, *Rev. Geophys.* **37**, 275 (1999).
8. S. Tilmes, R. Müller, A. Engel, M. Rex, J. M. Russell III, *Geophys. Res. Lett.* **33**, L20812 (2006).
9. M. von Hobe *et al.*, *Geophys. Res. Lett.* **33**, L17815 (2006).
10. J. J. Jin *et al.*, *Geophys. Res. Lett.* **33**, L15801 (2006).
11. M. Rex *et al.*, *Geophys. Res. Lett.* **33**, L23808 (2006).
12. EESC is an index that represents the temporal evolution of the chlorine- and bromine-containing (i.e., halogen-containing) gases in the stratosphere. The index accounts for projections of future abundances, the atmospheric lifetime of organic source molecules, and the relative efficiency of ozone loss by chlorine and bromine compounds (*13*). Here, a mean age of 5.5 years, appropriate for the polar regions, has been used (*13*).
13. P. A. Newman, J. S. Daniel, D. W. Waugh, E. R. Nash, *Atmos. Chem. Phys.* **7**, 4537 (2007).
14. S. Tilmes *et al.*, *J. Geophys. Res.* **112**, D24301 (2007).
15. K. Drdla, paper presented at the American Geophysical Union Fall Meeting, San Francisco, 5 to 9 December 2005.
16. L. Thomason, T. Peter, Eds. *Assessment of Stratospheric Aerosol Properties* (report no. 4, Stratospheric Process and Their Role in Climate, World Climate Research Programme 124, World Meteorological Organization/ TD-No. 1295, Toronto, 2006).
17. SAD is proportional to sulfate mass/r_{mode}, where r_{mode} is particle mode radius. The large-aerosol case assumes a similar perturbation to sulfate mass as the small-aerosol case. Therefore, the r_{mode} of the latter case, which is one-third as small as that of the former case, will result in a three times larger perturbation to SAD (*21*). Our estimate of SAD is derived from scaling the Mount Pinatubo perturbation based on information in (*1*, *2*).
18. G. A. Meehl *et al.*, *Climate Change 2007: The Physical Science Basis. Contribution of Working Group I to the Fourth Assessment Report of the Intergovernmental Panel on Climate Change*, S. Solomon *et al.*, Eds. (Cambridge Univ. Press, Cambridge, 2007), chap. 10.
19. D. J. Hofmann, S. J. Oltmans, *J. Geophys. Res.* **98**, 18,555 (1993).
20. G. Stenchikov *et al.*, *J. Geophys. Res.* **107**, 4803 (2002).
21. M. P. Chipperfield, V. E. Fioletov, in *Scientific Assessment of Ozone Depletion: 2006* (report no. 50, Global Ozone Research and Monitoring Project, World Meteorological Organization, Geneva, 2007), chap. 3.
22. S. Solomon *et al.*, *J. Geophys. Res.* **101**, 6713 (1996).

23. We acknowledge K. Drdla for helpful discussions and for sharing her formula to calculate T_{ACl} and PACl (*14*), P. Rasch for a very helpful discussion about the SAD distributions, and the UK Meteorological Office for providing meteorological analyses. The University Corporation for Atmospheric Research (UCAR) supported the portion of this work conducted at NCAR and the NASA Atmospheric Composition, Modeling, and Analysis Program supported the portion of this work conducted at the University of Maryland.

Supporting Online Material

www.sciencemag.org/cgi/content/full/1153966/DC1
SOM Text
Figs. S1 to S3
References

10 December 2007; accepted 9 April 2008
Published online 24 April 2008;
10.1126/science.1153966
Include this information when citing this paper.

Water Activity and the Challenge for Life on Early Mars

Nicholas J. Tosca,[1]* Andrew H. Knoll,[1] Scott M. McLennan[2]

In situ and orbital exploration of the martian surface has shown that acidic, saline liquid water was intermittently available on ancient Mars. The habitability of these waters depends critically on water activity (a_{H_2O}), a thermodynamic measure of salinity, which, for terrestrial organisms, has sharply defined limits. Using constraints on fluid chemistry and saline mineralogy based on martian data, we calculated the maximum a_{H_2O} for Meridiani Planum and other environments where salts precipitated from martian brines. Our calculations indicate that the salinity of well-documented surface waters often exceeded levels tolerated by known terrestrial organisms.

Because liquid water is required by all organisms on Earth, evidence of current or past water has been viewed as a first-pass filter for habitable environments on Mars. Further evaluation of habitability, however, requires that we move beyond the mere presence of water to consider its properties. Water may be required for life on Earth, but not all terrestrial waters are habitable; the limits of terrestrial life are defined by additional parameters, including temperature, pH, and salinity (*1*).

Layered martian rocks exposed on the Meridiani plain have been interpreted as sandstones containing Mg sulfate, Ca sulfate, jarosite [(K, Na, H_3O)$(Fe_{3-x}Al_x)(SO_4)_2(OH)_6$, where $x < 1$], and hematite (*2*–*5*). The geochemical, textural, and sedimentological features of these rocks are consistent with deposition in an arid, predominantly eolian setting, with intermittent percolation of acidic, oxidizing, and saline groundwater (*4*, *5*). The orbiting spectrometers OMEGA and CRISM have identified other localities across the martian surface that boast thick successions of layered rock rich in Mg and Ca sulfates (*6*). Evaporite minerals in martian meteorites and Fe-sulfate–rich soils analyzed at Gusev Crater provide still further evidence for acid saline conditions (*7*, *8*). By itself, the low pH inferred for martian brines need not have imposed a barrier to life (*1*). What, however, were the consequences of salinity?

At the high solute concentrations needed to form evaporite minerals, water is, to a large degree, made chemically unavailable by ion hydration. As a result, with increasing salinity, biological activity sharply decreases. Quantitatively, the chemical availability of liquid water can be expressed in terms of its activity (a_{H_2O}) (*9*). The a_{H_2O} of pure water is 1.0, a value that decreases with increasing

salinity. The a_{H_2O} of terrestrial seawater is 0.98, and the a_{H_2O} of most waters weathering Earth's continental crust falls between 0.98 and 1.0. Most organisms cannot grow at $a_{H_2O} \sim 0.9$, and few are known to tolerate $a_{H_2O} < 0.85$ (*10*). A few extreme eukaryotes fungi and archaea can live in NaCl-saturated solutions with an $a_{H_2O} = 0.75$ (*10*), and a single fungus, *Xeromyces bisporus*, has been shown to grow at $a_{H_2O} = 0.61$ in a high-sugar food (*10*, *11*). This represents the effective habitability limit for terrestrial organisms, but the biological stresses of organic solutes differ from those imposed by inorganic salts, and so the limiting a_{H_2O} could be higher for organisms in inorganic saline systems (*10*). Recently improved thermodynamic models allow us to calculate a_{H_2O} for martian surface environments and so constrain the probability that life arose and persisted there (*12*).

As evaporation proceeds, precipitating saline minerals act as robust markers for ambient a_{H_2O}. The sequence of precipitating minerals is itself controlled by the chemistry of initially dilute waters at the outset of evaporation (*13*). Because fluids on Mars chemically weathered a basaltic crust, the chemistry of dilute martian waters would have been distinct from that of most waters on Earth (*14*). Constraints on the cation chemistry associated with this process come largely from experimental and theoretical studies on the chemical weathering of martian basalt (*15*) [supporting online material (SOM) text].

Our results show that the evaporation of dilute martian waters results in distinct saline mineral assemblages, causing some minerals that are common in terrestrial settings to precipitate at lower a_{H_2O} values than they do on Earth (*16*). For example, halite does not precipitate from martian waters until $a_{H_2O} \leq 0.50$ because of the low abundance of Na released from basaltic weathering. On this basis, the identification of halite at the martian surface (*17*) indicates extreme salinity and brines that would not be inhabitable by known terrestrial organisms.

Temperature and anion content also control the a_{H_2O} of martian brines. The effect of temperature is minor near a temperature (T) > 0°C; a_{H_2O} might increase by ~0.03 to 0.05 over the range of 25° to 0°C. When freezing occurs and equilibrium between ice and surrounding brine is maintained, a_{H_2O} will be controlled by temperature and the amount of ice formed. Thus, in water ice–bearing areas on Mars, the a_{H_2O} of brine phases can be predicted by temperature alone (*18*) (fig. S4).

The proportional anion abundances of dilute evaporating waters exert one of the largest controls on a_{H_2O}. Unlike the principal cations in martian brines, major anions originate ultimately from volcanic degassing. At Meridiani, in situ chemical analyses suggest that the initial S/Cl molar ratio of groundwater brines ranged from ~6.0 to 30.0 (*19*). Here we focus on three important anion species and how changing their relative proportion before evaporation affects a_{H_2O}. Our calculations show that the effect of the SO_4/Cl ratio is most important, so that a decreasing ratio leads to progressively lower a_{H_2O} upon evaporative concentration (*20*) (fig. S1). We calculate that for martian waters with an initial molar SO_4/Cl = 6.0, halite precipitates when $a_{H_2O} = 0.48$. At a SO_4/Cl ratio of 1.0, halite precipitates when the $a_{H_2O} = 0.39$.

For Meridiani Planum, a_{H_2O} can be constrained separately for evaporation that occurred before sediment transport and deposition (Fig. 1) and for brine evolution during diagenesis. Evaporating fluids were initially generated by basaltic weathering (*14*); all major products initially formed by evaporation are probably represented in the Meridiani outcrop because its bulk composition is largely basaltic (*4*, *14*).

The initially precipitated Mg sulfate phase is not precisely identified in Meridiani rocks. Orbital spectroscopy of the surrounding region has identified kieserite ($MgSO_4 \cdot H_2O$) and other polyhydrated sulfates, for which a number of Mg sulfate hydrates are candidates (*6*). Because of this uncertainty, we considered the a_{H_2O} associated with the precipitation of various Mg sulfate hydrates (*21*). Epsomite precipitation places a maximum on a_{H_2O} at 0.78 (Fig. 1), with hexahydrite and kieserite precipitating at 0.62 and 0.51, respectively (SOM text). Because it represents the most conservative case with respect to habitability, we focus on epsomite here.

Diagenetic events at Meridiani are recorded by detailed textures viewed with the Microscopic Imager. Secondary crystal moldic porosity (or "vugs") in some beds records the syndepositional growth and subsequent dissolution of a soluble mineral. This mineral was preferentially removed by infiltrating groundwater, but much of the primary sedimentary fabric was preserved (Fig. 2). From these textures and the observation of abundant Mg sulfate in the outcrop, we infer that groundwater was at or near saturation with respect to a soluble Mg sulfate mineral (*4*, *14*). The infiltration of dilute water would largely have removed this soluble component, obliterating sedimentary features, which did not occur (Fig. 2). Instead, a variety of recrystallization textures and multiple generations of cement were left behind (*4*).

It has been suggested that the moldic porosity in Meridiani sediments reflects oxidation of a syndepositional Fe^{2+}-sulfate mineral such as melanterite ($Fe^{2+}SO_4 \cdot 7H_2O$) (*4*, *14*). Our calculations show that at 25°C, saturation with respect to epsomite and melanterite in this system occurs at an $a_{H_2O} = 0.78$, similar to the evaporation sequence described above. Oxidation of the soluble Fe^{2+} component to Fe^{3+}-bearing oxides and sulfates (i.e., jarosite) has the overall effect of increasing the a_{H_2O} to 0.86 while still maintaining epsomite saturation. Alternatively, the incongruent melting of meridianiite ($MgSO_4 \cdot 11H_2O$) to epsomite and water has been proposed as a mechanism for creating moldic porosity (*22*). The presence of this mineral before deposition and diagenesis

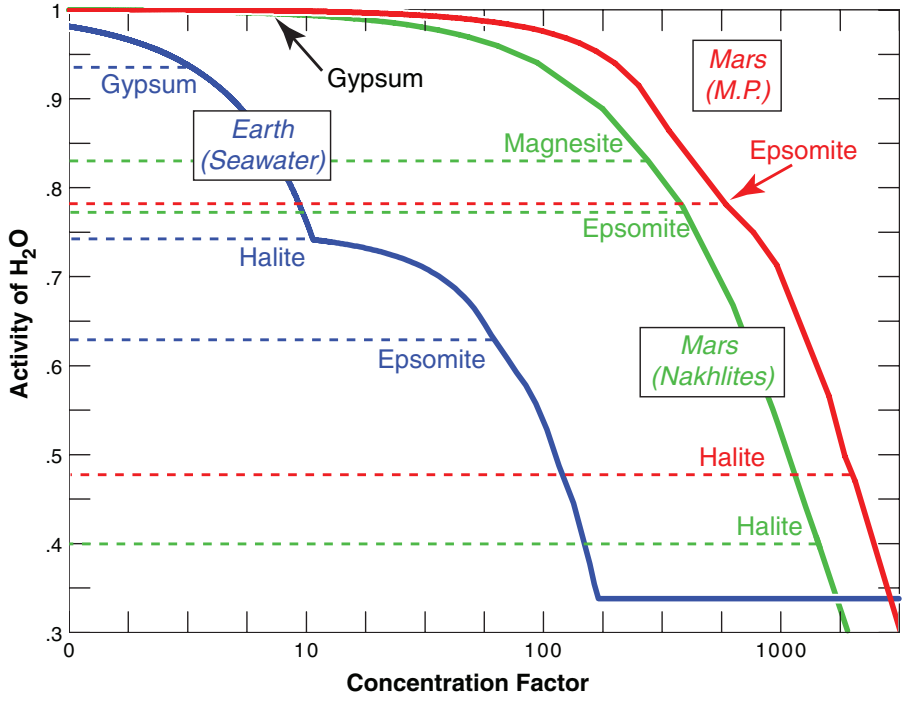

Fig. 1. Calculated mineral precipitation and a_{H_2O} values as a function of evaporative concentration. The blue line represents modern terrestrial seawater evaporation. The red line represents the evaporation of a basaltic-weathering derived fluid most representative of inferred evaporation processes at Meridiani Planum. The green line represents the evaporation of a similar fluid but with an anion concentration that gives rise to the saline mineral assemblage observed in the Nakhla meteorite (and other members of the nakhlite meteorite class).

[1]Department of Organismic and Evolutionary Biology, Harvard University, Cambridge, MA 02138, USA. [2]Department of Geosciences, State University of New York, Stony Brook, NY 11794, USA.

*To whom correspondence should be addressed. E-mail: ntosca@fas.harvard.edu

requires the freezing of aqueous fluids. Water ice is likely to have formed in association with this process, appearing at temperatures near 0°C (*18*). If water ice melts, the brine composition approaches a chemical state essentially identical to the epsomite calculation described above, with an $a_{H_2O} = 0.78$ at epsomite and melanterite saturation.

Late-stage chloride precipitates have also been explored as vug precursor minerals on the basis of their relatively high solubility (*19*). Regardless of its identity, the dissolution of a chloride phase would require that infiltrating pore water became less saline, but still attained saturation with respect to Mg sulfate, with epsomite again fixing a_{H_2O} at 0.78.

Taken together, our results indicate that the evaporation of Meridiani groundwater led to a sustained $a_{H_2O} \leq 0.78$ to 0.86, values too low for all but a handful of terrestrial microorganisms to survive. Moreover, additional evidence suggests that chlorides are present in the sediments, pointing to still lower a_{H_2O} with continuing brine evolution. A range of Br/Cl ratios in different rocks suggests that highly soluble chlorides formed from evaporation and were incorporated into the wind-blown sediments (*4*, *19*). Progressive increases in Cl in rocks deeper in Endurance Crater suggest a similar process or one that differentially affected Cl during diagenesis (*19*). In addition, there is chemical and textural evidence for halite on rinds and rock coatings analyzed at Meridiani Planum, most likely reflecting late-stage fluid movement or remnants left when altering fluids finally evaporated to dryness (*23*). Accordingly, the maximum a_{H_2O} at chloride formation (0.48, Fig. 1) may reflect initial evaporite formation, syndepositional fluid chemistry, and/or very late-stage diagenesis.

On a planetary scale, Mars Odyssey Gamma Ray Spectrometer results show Cl-H_2O correlation across much of the martian surface (*24*), consistent with recent spectral evidence for widespread mid- to late-Noachian chloride-bearing lithologies in the southern highlands (*25*). Because late-stage martian brines would have evolved toward Cl-rich compositions as sulfates were precipitated (*20*), these observations probably represent the signature of low-a_{H_2O} brines. "Paso Robles"–class Fe-sulfate–rich soils at Gusev Crater represent another investigated locality characterized by extreme acidity and high salinity (*8*). Mössbauer and reflectance spectroscopic measurements, supported by α-proton x-ray spectrometer analyses, show that candidate Fe-sulfate minerals include ferricopiapite and rhomboclase (*8*, *26*, *27*). Mg sulfate is also indicated in some analyses, occurring as several percent $MgSO_4$ by weight. The a_{H_2O} for a Fe^{3+}-rich brine in equilibrium with ferricopiapite, rhomboclase, and epsomite is 0.61, with a pH (SOM text) of –0.7: a remarkably harsh environment uninhabitable by known microorganisms (*10*, *18*).

Some martian meteorites also contain evaporite assemblages of martian origin, most likely reflecting subsurface geochemical processes. Members of the nakhlite class have carbonate minerals, including siderite and magnesite, as well as gypsum and epsomite (*7*). The Nakhla meteorite also contains late-stage halite; its saline assemblage represents the highest recorded extent of evaporative concentration on Mars. This evaporite mineral assemblage can be generated from an acidic solution with the same cation proportions as at Meridiani Planum (setting an initial pH of 4.8 and a SO_4/Cl ratio of 2.05) (*20*). After siderite and gypsum precipitate, magnesite appears at an a_{H_2O} of 0.83, then epsomite at $a_{H_2O} = 0.78$. Halite precipitates at an a_{H_2O} of 0.40 (Fig. 1). These calculations imply that the a_{H_2O} of at least some fluids percolating through the martian subsurface dipped well below known limits of terrestrial habitability.

Our calculations suggest that a number of martian localities widely distributed in time and space hosted fluids that were 10 to 100 times more saline than halite-saturated terrestrial seawater. A number of terrestrial organisms have evolved mechanisms to accommodate the osmotic stresses imposed by high salinities (*28*). However, all known salt-tolerant organisms are descended from ancestors that could not survive low a_{H_2O}, indicating that although life has evolved mechanisms to stretch the envelope of habitability, such brines were not a cradle for life on Earth (*1*, *10*, *28*). Accordingly, life that could originate and persist in the presence of extremely low a_{H_2O} on Mars would require biochemistry distinct from any known in even the most robust halophiles on Earth.

Precipitation is the sedimentary signature of brines with low a_{H_2O}; dissolution records more dilute waters. Although more dilute solutions must have carried ions to the sites where Meridiani salts precipitated, there is little evidence locally that subsequent water table regeneration introduced groundwaters dilute enough to dissolve Mg-sulfate minerals. Globally, we cannot rule out the possibility that more habitable waters existed elsewhere on the planet or in the earliest epoch of martian history. However, empirical evidence for dilute water at the martian surface remains meager. Geochemical constraints on Meridiani diagenesis suggest that the process was limited by the availability of water (*29*), which is consistent with a global surface geochemistry controlled for more than 3.5 billion years by water-limited processes (*30*). At the same time, hydrological models suggest that Meridiani Planum was one of the few regions on Mars likely to be characterized by groundwater upwelling about four billion years ago (*31*). This slow, global-scale deep hydrology would have focused water/rock interactions on the subsurface, leading to chemically distinct, concentrated groundwaters (*31*). When migrating groundwater breached the surface, continued upwelling and evaporation would have allowed standing water bodies to evolve toward greater ionic concentrations while keeping total fluid volume more or less constant. Concentrated standing water left its mark at Meridiani Planum in the form of diagnostic subaqueous cross-beds (*2*, *4*, *5*), and these same rocks display some of the highest MgO and SO_3 abundances measured, implying Mg-sulfate saturation and low a_{H_2O}. Moreover, the search for larger, more dilute bodies of water earlier in the Noachian has proven difficult (*25*, *32*). New observations have abbreviated the era when dilute surface waters could have been more common, pushing it further into Mars' planetary infancy.

Observations at Meridiani and other salt-bearing localities, then, may not reflect snapshots taken as local Mars waters evaporated to dryness, but rather a long surface history dominated by rock instead of water. On a planet where saline minerals were continuously recycled at the surface instead of removed by subduction and plate tectonics, dilute fluids may have been transient exceptions. The sobering conclusion is that Meridiani Planum, an extreme environment in terms of terrestrial habitability, may have been among the last, best places for life on the early martian surface.

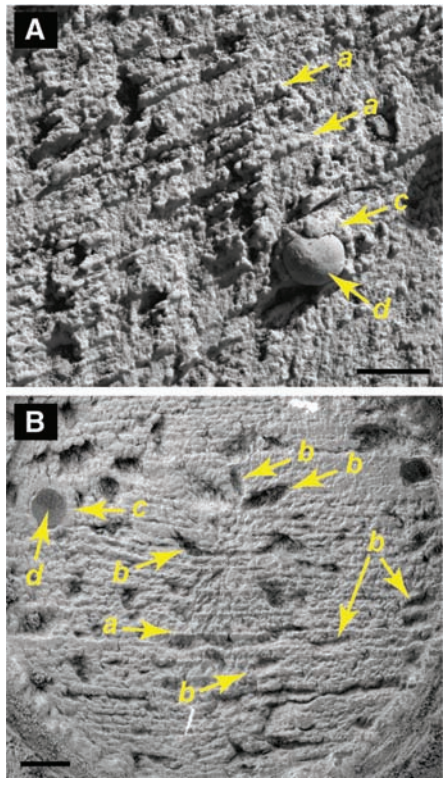

Fig. 2. Microscopic images taken by the Mars Exploration Rover Opportunity in Endurance Crater. (**A**) Portion of image taken of the undisturbed surface of Cobble Hill on martian day (sol) 144. (**B**) Portion of a mosaic taken on sol 149 of the feature London after being ground with the rock abrasion tool (RAT). Distinct grain boundaries are observable throughout both images. Primary laminations (a) and bedding structures are clearly visible. Secondary moldic porosity (b) can be seen throughout the RAT-abraded target, providing evidence for the selective removal of a syndepositionally formed soluble mineral while preserving primary sedimentary fabric. These features, observable in most places throughout Meridiani outcrop rocks, suggest groundwater saturation with respect to a Mg-sulfate phase during diagenesis. Secondary recrystallization is evident in some places, as shown by a generation of cement (c) surrounding hematitic concretions (d). Scale bars, 5 mm.

References and Notes

1. A. H. Knoll *et al.*, *Earth Planet. Sci. Lett.* **240**, 179 (2005).
2. S. W. Squyres *et al.*, *Science* **306**, 1709 (2004).
3. G. Klingelhöfer *et al.*, *Science* **306**, 1740 (2004).
4. S. M. McLennan *et al.*, *Earth Planet. Sci. Lett.* **240**, 95 (2005).
5. J. P. Grotzinger *et al.*, *Earth Planet. Sci. Lett.* **240**, 11 (2005).
6. A. Gendrin *et al.*, *Science* **307**, 1587 (2005).
7. J. C. Bridges, M. M. Grady, *Earth Planet. Sci. Lett.* **176**, 267 (2000).
8. D. W. Ming *et al.*, *J. Geophys. Res. Planets* **111**, E02S12 (2006).
9. At equilibrium, the vapor pressure of water above an aqueous solution is equal to p_{aq}. For pure water at a standard state, the vapor pressure is equal to p_f^0. The activity of the solvent water, a_{H_2O}, is given by $a_{H_2O} = \frac{p_{aq}}{p_f^0}$.
10. W. D. Grant, *Philos. Trans. R. Soc. London Ser. B* **359**, 1249 (2004).
11. The food industry has expended considerable effort to characterize biological limits to a_{H_2O} in order to retard spoilage by microbial growth. The paucity of organisms found at low a_{H_2O} represents biological limitation rather than sampling or research bias.
12. Methods are described in the SOM text.
13. L. A. Hardie, H. P. Eugster, *Mineral. Soc. Am. Spec. Pub.* **3**, 273 (1970).
14. N. J. Tosca *et al.*, *Earth Planet. Sci. Lett.* **240**, 122 (2005).
15. N. J. Tosca *et al.*, *J. Geophys. Res. Planets* **109**, E05003 (2004).
16. Our calculations simulate the evaporation of a dilute basaltic-weathering derived fluid. Equilibrium with a 1-bar CO_2 atmosphere is maintained; the SO_4/Cl is specified; and pH, initially 3.9 unless otherwise stated, is calculated by charge balance.
17. Sedimentary redistribution may complicate estimations of a_{H_2O} for specific localities.
18. G. M. Marion, J. S. Kargel, *Cold Aqueous Geochemistry with FREZCHEM* (Springer-Verlag, Berlin, 2008).
19. B. C. Clark *et al.*, *Earth Planet. Sci. Lett.* **240**, 73 (2005).
20. N. J. Tosca, S. M. McLennan, *Earth Planet. Sci. Lett.* **241**, 21 (2006).
21. Relative humidity (RH) or brine chemistry may affect the hydration state of some evaporitic minerals. Here we exclude postdepositional RH effects and consider only fluid evaporation.
22. R. C. Peterson, R. Y. Wang, *Geology* **34**, 957 (2006).
23. A. H. Knoll *et al.*, *J. Geophys. Res. Planets* **113**, E06S16 (2008).
24. J. M. Keller *et al.*, *J. Geophys. Res. Planets* **111**, E03S08 (2006).
25. M. M. Osterloo *et al.*, *Science* **319**, 1651 (2008).
26. J. R. Johnson *et al.*, *Geophys. Res. Lett.* **34**, L13202 (2007).
27. Mössbauer spectra show that candidate minerals must be Fe-sulfates distinct from jarosite. At such highly concentrated and acidic conditions, the a_{H_2O} is relatively insensitive to the exact Fe-sulfate phase (see SOM).
28. A. Oren, *J. Ind. Microbiol. Biotechnol.* **28**, 56 (2002).
29. M. E. Elwood-Madden, R. J. Bodnar, J. D. Rimstidt, *Nature* **431**, 821 (2004).
30. J. A. Hurowitz, S. M. McLennan, *Earth Planet. Sci. Lett.* **260**, 432 (2007).
31. J. C. Andrews-Hanna, R. J. Phillips, M. T. Zuber, *Nature* **446**, 163 (2007).
32. M. H. Carr, *The Surface of Mars* (Cambridge Univ. Press, New York, 2007).

33. We thank the MER science and engineering teams for measurements of martian materials that made this paper possible. Research supported in part by NASA and a Harvard Origins postdoctoral fellowship to NJT.

Supporting Online Material

www.sciencemag.org/cgi/content/full/320/5880/1204/DC1
SOM Text
Figs. S1 to S4
Tables S1 to S6
References

18 January 2008; accepted 18 April 2008
10.1126/science.1155432

A Cytosolic Iron Chaperone That Delivers Iron to Ferritin

Haifeng Shi,[1] Krisztina Z. Bencze,[2] Timothy L. Stemmler,[2] Caroline C. Philpott[1]*

Ferritins are the main iron storage proteins found in animals, plants, and bacteria. The capacity to store iron in ferritin is essential for life in mammals, but the mechanism by which cytosolic iron is delivered to ferritin is unknown. Human ferritins expressed in yeast contain little iron. Human poly (rC)–binding protein 1 (PCBP1) increased the amount of iron loaded into ferritin when expressed in yeast. PCBP1 bound to ferritin in vivo and bound iron and facilitated iron loading into ferritin in vitro. Depletion of PCBP1 in human cells inhibited ferritin iron loading and increased cytosolic iron pools. Thus, PCBP1 can function as a cytosolic iron chaperone in the delivery of iron to ferritin.

Ferritins are iron storage proteins that are ubiquitously expressed in animals, plants, and bacteria. They serve both to sequester excess iron taken up by the cell and to release stored iron to meet the cell's metabolic needs during iron scarcity (*1*). In animals, ferritin is a cytosolic heteropolymer consisting of 24 subunits of heavy (H) and light (L) isoforms that assemble into a hollow sphere into which iron is deposited. Ferritin H chains contain the iron-binding and ferroxidase activities that are required for mineralization of the ferritin core. Deletion of the H-ferritin gene is lethal in mice (*2*) and in flies (*3*).

In cells, metallochaperones deliver metals to their cognate enzymes and transporters. Although cytosolic copper and nickel chaperones have been described (*4*–*7*), no cytosolic iron chaperones have been identified, despite the presence of numerous iron-dependent enzymes in the cytosol. Frataxin—the protein lacking in the neurological disease Friedreich's ataxia—functions as a mitochondrial iron chaperone for iron-sulfur cluster and heme biosynthesis (*8*, *9*).

Fungi are anomalous among eukaryotes in that they do not express ferritins. We expressed human H and L ferritins in the yeast *Saccharomyces cerevisiae*. The peptides assembled into multimeric complexes, with properties similar to those of native human ferritins, but contained only small amounts of iron (fig. S1, A and B). We hypothesized that yeast might also lack the requisite iron chaperones needed for delivery of iron to ferritin and designed a genetic screen to identify human genes that, when expressed in yeast, could increase the amount of iron loaded into ferritin. We introduced an iron-regulated *FeRE*/*HIS3* reporter construct (*10*) into a yeast strain expressing H and L ferritin (Fig. 1A). This construct confers histidine prototrophy to cells when the reporter is bound and transcriptionally activated by Aft1p, the major iron-dependent transcription factor in yeast. Aft1p is activated during periods of cytosolic iron depletion (*11*), which could occur if substantial amounts of cytosolic iron were diverted into ferritin.

Yeast cells containing ferritin and the iron-responsive reporter were transformed with a library synthesized from human liver cDNA engineered into a yeast expression vector. Transformants that exhibited growth on plates lacking histidine were selected for further analysis. We isolated multiple copies of PCBP1, as well as proteins encoded by other unrelated genes, including H ferritin. Plasmids containing PCBP1 or the empty vector were retransformed into reporter yeast strains lacking or expressing H and L ferritins (Fig. 1B). Expression of PCBP1 did not activate the *FeRE*/*HIS3* reporter in cells lacking ferritin, as indicated by a lack of growth on media without histidine. But expression of PCBP1 did activate the *FeRE*/*HIS3* reporter in the yeast strain expressing ferritins, resulting in growth on media lacking histidine. Thus, expression of human PCBP1 activated the iron-responsive reporter only in the presence of ferritin. To confirm that reporter activation was due to delivery of cytosolic iron into ferritin, we directly measured the incorporation of iron into ferritin by growing yeast in the presence of $[^{55}Fe]Cl_3$, isolating ferritin on nondenaturing gels, and measuring the amount of ^{55}Fe in the ferritin heteropolymer (Fig. 1, C and D). Substantial amounts of iron-containing protein were detected only in cells expressing ferritin, and iron was detected in a single species that comigrated with the ferritin heteropolymer. Coexpression of PCBP1 in these cells resulted in a 2.3-fold increase in the amount of iron in ferritin. This increase was not due to changes in the overall amount of ferritin (Fig. 1E) or in the relative ratio of H and L chains (fig. S1A). Similarly, the total amount of ^{55}Fe taken up by the cells expressing ferritin alone was not different from the amount taken up by cells expressing both PCBP1 and ferritin (fig. S1C).

The delivery of cytosolic iron to ferritin in the presence of PCBP1 activated the *FeRE*/*HIS3* reporter. We asked whether other proteins ex-

[1]Liver Diseases Branch, National Institute of Diabetes and Digestive and Kidney Diseases, National Institutes of Health, Bethesda, MD 20892, USA. [2]Department of Biochemistry and Molecular Biology, Wayne State University School of Medicine, Detroit, MI 48201, USA.

*To whom correspondence should be addressed. E-mail: carolinep@intra.niddk.nih.gov